

Structural determination by single-molecule vibrational spectroscopy and microscopy: Contrast between copper and iron carbonyls

H. J. Lee and W. Ho*

Laboratory of Atomic and Solid State Physics and Cornell Center for Materials Research, Cornell University, Ithaca, New York 14853

(Received 5 April 2000)

A scanning tunneling microscope (STM) was used to synthesize $\text{Cu}(\text{CO})$, $\text{Fe}(\text{CO})$, $\text{Cu}(\text{CO})_2$, and $\text{Fe}(\text{CO})_2$ from individual Cu atoms, Fe atoms, and CO molecules on a $\text{Ag}(110)$ surface at 13 K. Inelastic electron tunneling spectroscopy and microscopy together with topographical imaging revealed contrasting bonding geometries for the single Cu and Fe carbonyl products.

Dissociation of individual molecules with a scanning tunneling microscope (STM) on semiconductor^{1,2} and metal^{3,4} surfaces has successfully demonstrated the use of the STM as a tool for chemical transformation of matter on the atomic scale. Currently, the precision of STM-induced dissociation is such that single bond scission could be achieved in a polyatomic molecule while leaving another identical bond intact.⁵ The reverse process of single bond formation has also been realized.⁶ Chemical sensitivity of the STM provided by inelastic electron tunneling spectroscopy (STM-IETS) (Ref. 7) enabled identification and characterization of the products of single-molecule dissociation^{4,5} and synthesis.⁶ These capabilities of the STM, combined with manipulation,⁸⁻¹⁰ are expected to contribute to the development of nanoscale materials and devices.

In the present work, we used a low temperature STM operating in ultrahigh vacuum¹¹ to synthesize chemical species on the surface and to characterize the reactants and products with spatial imaging and vibrational spectroscopy and microscopy. Starting with a clean $\text{Ag}(110)$ surface at 13 K, individual Cu atoms and Fe atoms were first evaporated onto the surface, followed by adsorption of two isotopes of CO ($^{12}\text{C}^{16}\text{O}$ and $^{13}\text{C}^{18}\text{O}$) from the gas phase. To prevent interactions between coadsorbed species, exposures of Cu, Fe, and CO isotopes were limited to yield coverages of ~ 0.001 monolayer. In topographical images taken at 70 mV sample bias and 1 nA tunneling current, Cu and Fe atoms appeared as protrusions of 0.48 Å and 0.83 Å, respectively. Both CO isotopes appeared as depressions of -0.30 Å. Images of all these species exhibited azimuthal symmetry.

The controlled formation of a Cu-CO (Fe-CO) bond consists of a series of systematic steps with the STM.⁶ The STM feedback remains on throughout the process. After taking a topographical image of the surface at 70 mV sample bias and 0.1 nA tunneling current, the tip is positioned over a CO molecule. The bias voltage is increased to 250 mV and the tunneling current is ramped to 10 nA to induce the transfer of the CO molecule to the tip. The bias and tunneling current are then reduced to 70 mV and 0.1 nA, and the tip is translated and positioned over a Cu (Fe) atom. The Cu-CO (Fe-CO) bond is formed by first changing the bias to -70 mV, followed by increasing the tunneling current to 10 nA, and finally ramping the bias to about -7 mV (-4 mV for Fe-CO).

Using the above procedure, $\text{Cu}(\text{CO})$, $\text{Fe}(\text{CO})$, $\text{Cu}(\text{CO})_2$, and $\text{Fe}(\text{CO})_2$ molecules were formed on the surface with different CO isotopes.¹² The spatial resolution was increased in the topographical scans by attaching a CO molecule to the tip,⁶ allowing direct imaging of the Ag atoms and the determination of the adsorption sites: atop for the CO isotopes and fourfold hollow for Cu, Fe, and the carbonyl products (Fig. 1).

Symmetry in the topographical image of $\text{Cu}(\text{CO})$ shown in Fig. 2(a) implies that CO is bonded perpendicular to the surface [Figs. 2(c) and (d)]. The slight elongation in the image along the $[1\bar{1}0]$ direction reflects the underlying silver

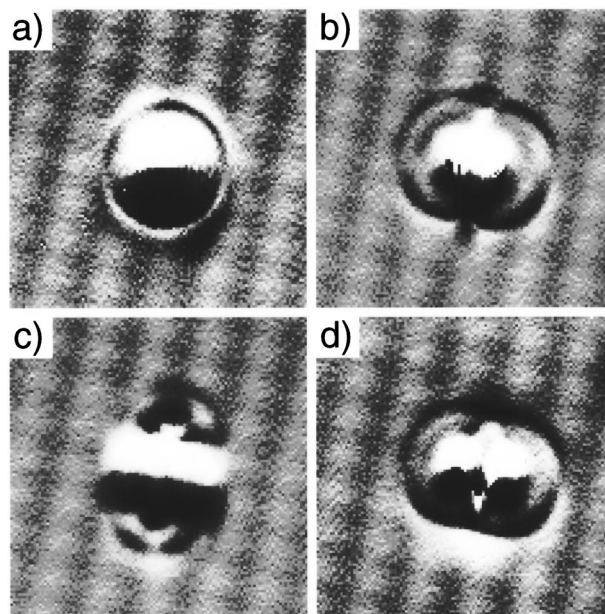


FIG. 1. Atomically resolved topographical images of (a) $\text{Cu}(\text{CO})$, (b) $\text{Fe}(\text{CO})$, (c) $\text{Cu}(\text{CO})_2$, and (d) $\text{Fe}(\text{CO})_2$ recorded at 70 mV sample bias and 2 nA tunneling current with a CO molecule attached to the tip. Size of each scan is $22 \times 22 \text{ \AA}^2$. Note that the image of $\text{Fe}(\text{CO})$ is a superposition of two possible orientations because of frequent flips of the CO molecule during the scan with these tunneling parameters. In these images, it is not the tip height (z) that is displayed but its derivative (dz/dy), where y is the scan direction (from top to bottom). This has the effect of illuminating the scan area from the top side of the image and accentuating small corrugations.

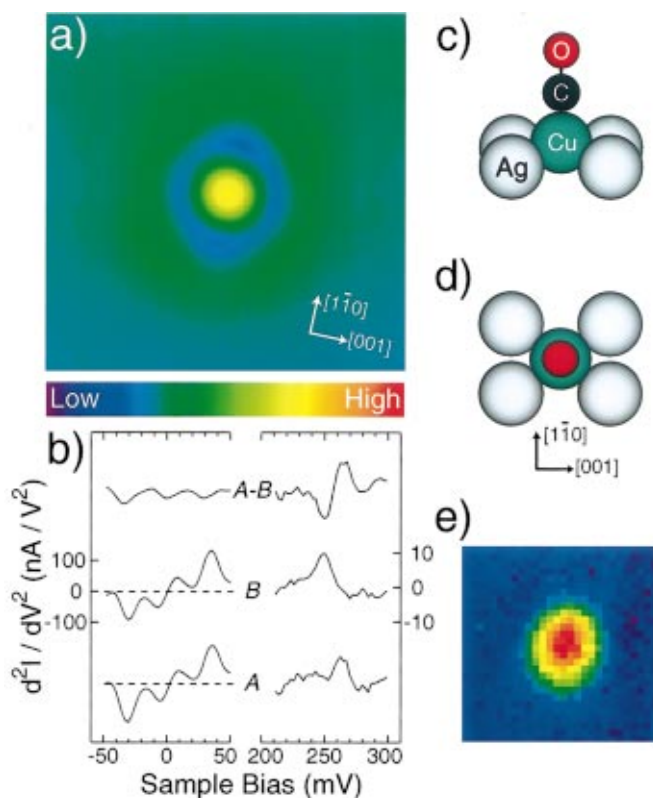


FIG. 2. (Color) (a) $25 \times 25 \text{ \AA}^2$ topographical image of $\text{Cu}(\text{CO})$ recorded at 70 mV sample bias and 1 nA tunneling current. The color bar shows the color scheme used to represent the tip height at each pixel point. The range of tip height shown in the color bar is from -0.20 \AA (violet) to $+0.46 \text{ \AA}$ (red) relative to the Ag surface. The same color bar is used in other figures. The underlying lattice orientation has been determined by scanning the area with a CO molecule attached to the tip (Fig.1). (b) (Line A) Single-molecule vibrational spectrum of $\text{Cu}({}^{12}\text{C}{}^{16}\text{O})$. Background spectrum over the bare Ag surface has been subtracted. (Line B) Background subtracted spectrum for $\text{Cu}({}^{13}\text{C}{}^{18}\text{O})$. (Line A-B) Difference between spectra A and B. The side view (c) and top view (d) of $\text{Cu}(\text{CO})$ show the CO ligand to be perpendicular to the surface as implied by the symmetry in the image (a) and the spatial distribution of the vibrational signal in (e). (e) Spatial distribution of d^2I/dV^2 at the C-O hindered rotation energy of $\text{Cu}(\text{CO})$ on Ag(110). Color palette is the same as the one in (a), but here the colors represent the d^2I/dV^2 signal: -12 nA/V^2 (violet) to $+92 \text{ nA/V}^2$ (red). Scan size is $14 \times 14 \text{ \AA}^2$ with 0.5 \AA pixel resolution.

lattice. Single-molecule vibrational spectroscopy by STM-IETS provides chemical identification of the bonding. Details of STM-IETS have been described elsewhere.^{7,11,13} For $\text{Cu}({}^{12}\text{C}{}^{16}\text{O})$, a C-O stretch mode at 262 meV and a C-O hindered rotation mode at 36 meV (-32 meV for negative sample bias) are observed [Fig. 2(b), line A]. These vibrational modes are shifted down to 249 meV and 34 meV (-31 meV for negative sample bias), respectively, for $\text{Cu}({}^{13}\text{C}{}^{18}\text{O})$ [Fig. 2(b), line B].

In contrast, two orientations were observed for $\text{Fe}(\text{CO})$. One orientation is shown in Fig. 3(a) and the other orientation is a mirror image reflected about the plane containing $[1\bar{1}0]$. This asymmetry in the image suggests that the CO ligand in $\text{Fe}(\text{CO})$ is tilted, bent, or has both tilt and bent angles. To determine the relation of the lobe to the CO mol-

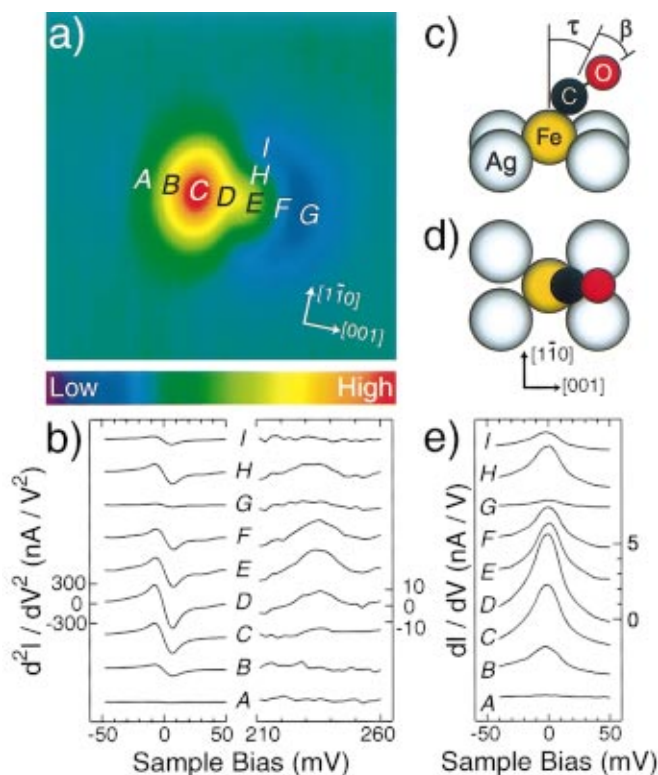


FIG. 3. (Color) (a) $25 \times 25 \text{ \AA}^2$ image of $\text{Fe}(\text{CO})$ recorded at 70 mV and 1 nA. Letters A through I denote the tip position for the corresponding vibrational spectra shown in (b). (b) Spatially resolved, background subtracted single-molecule vibrational spectra of $\text{Fe}(\text{CO})$. The side view (c) and top view (d) of $\text{Fe}(\text{CO})$ show the CO to be tilted by angle τ and bent by angle β as suggested by the asymmetry in the image (a) and the spatial distribution of the vibrational signal in (b). (e) Background subtracted dI/dV spectra recorded over the positions labeled in (a).

ecule, we placed the STM tip at various locations in the image and recorded the vibrational spectra by STM-IETS [Fig. 3(b)]. The spatial distribution of the C-O stretch signal at 236 meV determines that the CO ligand in $\text{Fe}(\text{CO})$ is inclined and gives rise to the side lobe in the topographical image [Figs. 3 (a), (c), and (d)]. A quantitative determination of the tilt and bent angles requires theoretical calculations.

The symmetry in the topographical image of $\text{Cu}(\text{CO})_2$ [Fig. 4(a)] implies that the two CO ligands are symmetrically located on the Cu atom, but the orientation of the CO ligands cannot be determined from the image alone. The presence of two mirror planes in the image is consistent with either of the two sets of orientations 90° away (A and B vs C and D). Unambiguous determination of molecular orientation can be accomplished by forming a molecule with mixed isotopes, $\text{Cu}({}^{12}\text{C}{}^{16}\text{O})({}^{13}\text{C}{}^{18}\text{O})$, and performing STM-IETS on different parts of the molecule [Fig. 4(b)]. The vibrational spectra taken at position A in Fig. 4(a) revealed the ${}^{12}\text{C}{}^{16}\text{O}$ stretch at 255 meV and the ${}^{12}\text{C}{}^{16}\text{O}$ hindered rotation at 35.5 meV (-34.3 meV for negative sample bias) [Fig. 4(b), line A]. At position B, peaks at 244 meV and 34.8 meV (-33.8 meV for negative bias) were recorded for the ${}^{13}\text{C}{}^{18}\text{O}$ stretch and hindered rotation, respectively [Fig. 4(b), line B]. On the other hand, spectra recorded over positions C and D are similar to each other. Therefore, we conclude that the molecular

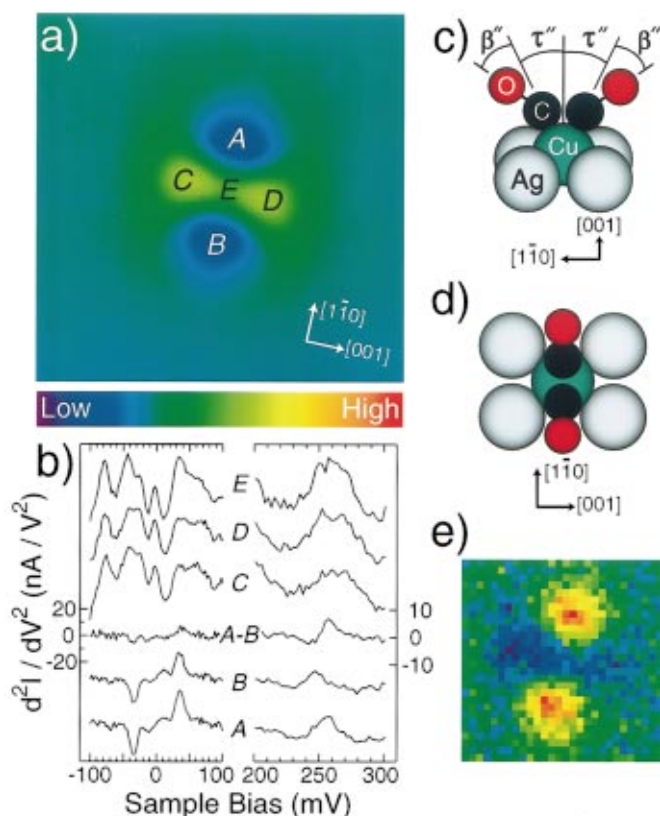


FIG. 4. (Color) (a) $25 \times 25 \text{ \AA}^2$ image of $\text{Cu}({}^{12}\text{C}^{16}\text{O})({}^{13}\text{C}^{18}\text{O})$ recorded at 70 mV and 1 nA. (b) Spatially resolved, background subtracted single-molecule vibrational spectra of $\text{Cu}({}^{12}\text{C}^{16}\text{O}) \times ({}^{13}\text{C}^{18}\text{O})$. Spectra A through E were recorded over the positions labeled in (a). The side view (c) and top view (d) of $\text{Cu}(\text{CO})_2$ show tilt-and-bent geometry with angles τ'' and β'' as suggested by the image (a) and the spatial distribution of the vibrational signal in (b) and (e). (e) Spatial distribution of d^2I/dV^2 at the C-O hindered rotation energy of $\text{Cu}(\text{CO})_2$ on $\text{Ag}(110)$. The color palette is the same as that of (a), but here the colors represent d^2I/dV^2 signal: -23 nA/V^2 (violet) to $+26 \text{ nA/V}^2$ (red). Scan size is $14 \times 14 \text{ \AA}^2$ with 0.5 \AA pixel resolution.

structure for $\text{Cu}(\text{CO})_2$ on $\text{Ag}(110)$ is as shown in Figs. 4(c) and (d). Vibrational microscopy of the hindered rotation in Fig. 4(e) provides further support of the structure. It is interesting to note that at positions C, D, and E, electronic contributions to the spectra are significantly different from that on the bare Ag surface, contrary to positions A and B where background subtracted spectra are nearly flat except for the vibrational features.

In the case of $\text{Fe}(\text{CO})_2$, the symmetry of the topographical image [Fig. 5(a)] implies that the two CO ligands are also symmetrically located on the Fe atom. Vibrational spectra for $\text{Fe}({}^{12}\text{C}^{16}\text{O})_2$ [Fig. 5(b)] show maximum intensity for C-O stretching mode at the center of the molecule because two identical CO ligands contribute to the intensity. As with the $\text{Cu}(\text{CO})_2$ case, a molecule with mixed isotopes, $\text{Fe}({}^{12}\text{C}^{16}\text{O})({}^{13}\text{C}^{18}\text{O})$, was formed to determine the molecular orientation. The ${}^{12}\text{C}^{16}\text{O}$ stretch at 235 meV and ${}^{13}\text{C}^{18}\text{O}$ stretch at 223 meV were revealed separately at each protrusion in the topographical image [Figs. 5(a) and (e)]. Therefore, we conclude that the geometry for $\text{Fe}(\text{CO})_2$ on $\text{Ag}(110)$ is as shown in Figs. 5(c) and (d).

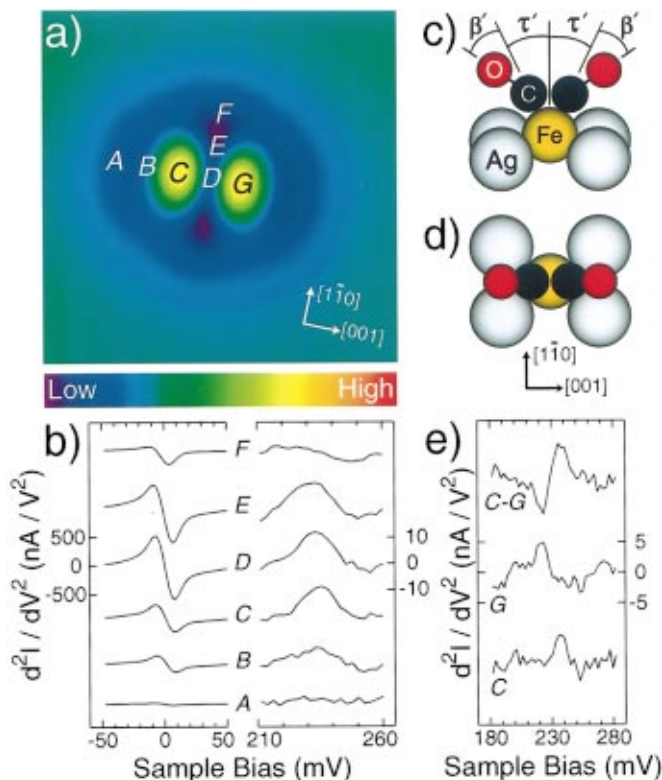


FIG. 5. (Color) (a) $25 \times 25 \text{ \AA}^2$ image of $\text{Fe}(\text{CO})_2$ recorded at 70 mV and 1 nA. (b) Background subtracted single-molecule vibrational spectra of $\text{Fe}({}^{12}\text{C}^{16}\text{O})_2$ recorded over the positions labeled in (a). The side view (c) and top view (d) of $\text{Fe}(\text{CO})_2$ show tilt-and-bent geometry with angles τ' and β' as suggested by the image (a) and the spatial distribution of the vibrational signal in (b) and (e). (e) Background subtracted vibrational spectra of $\text{Fe}({}^{12}\text{C}^{16}\text{O}) \times ({}^{13}\text{C}^{18}\text{O})$ taken over the left protrusion (line C) and right protrusion (line G). Difference between spectra C and G (line C-G). Spectra shown in (e) were taken with a tip different from the one used in (b), and therefore intensities cannot be directly compared.

The structures for Cu and Fe carbonyls show significant contrast: linear $[\text{Cu}(\text{CO})]$ versus inclined $[\text{Fe}(\text{CO})]$ structure for monocarbonyl products while the plane of the molecule for $\text{Cu}(\text{CO})_2$ and $\text{Fe}(\text{CO})_2$ are perpendicular to each other. The electronic properties of Cu and Fe are likely to be responsible for these different structures. Steric interactions of CO with the Ag atoms could also be important. Images obtained with CO attached to the tip show rings which are believed to be associated with the CO ligands; the locations of the rings in the images are consistent with the CO orientations (Fig. 1). Theoretical calculations are needed to fully understand the origin of the contrast in structure and bonding between Cu and Fe carbonyls.

The C-O stretch and C-O hindered rotation energies measured above for $\text{Cu}(\text{CO})$ and $\text{Cu}(\text{CO})_2$ are close to the STM-IETS results for CO on $\text{Cu}(001)$: 256 meV for ${}^{12}\text{C}^{16}\text{O}$ stretch, 244 meV for ${}^{13}\text{C}^{18}\text{O}$ stretch, 36.3 meV for ${}^{12}\text{C}^{16}\text{O}$ hindered rotation, and 35.2 meV for ${}^{13}\text{C}^{18}\text{O}$ hindered rotation.¹⁴ Also, the observed isotope shift of 13 meV between $\text{Cu}({}^{12}\text{C}^{16}\text{O})$ and $\text{Cu}({}^{13}\text{C}^{18}\text{O})$ is close to the calculated gas phase value of 11.8 meV.¹⁵ We note that the C-O hindered rotation energies for $\text{Cu}(\text{CO})$ and $\text{Cu}(\text{CO})_2$ show a dependence on the direction of tunneling current; the abso-

lute values of the peak positions at negative sample bias were always lower than those at positive bias. This shift was also observed for CO on Cu(001) and Cu(110), and the possibility of a Stark shift was systematically eliminated.¹⁴ Cu(CO) shows larger shift (~ 4 meV) than Cu(CO)₂ (~ 1 meV).

Detailed vibrational analysis of Fe carbonyl products has been described elsewhere.⁶ The C-O hindered rotation mode was not observed for Fe(CO) and Fe(CO)₂, but instead there were enhancements in the ac conductance (dI/dV) near zero bias [Fig. 3(e)], resulting in asymmetric line shape of the d^2I/dV^2 curves [Fig. 3(b) and Fig. 5(b)]. This resonance was not observed on a bare Fe atom adsorbed on Ag(110). Addition of a third CO on Fe(CO)₂ was observed to suppress the resonance. Further experimental and theoretical studies are needed in order to understand these results.

We have also examined the possibility of reversing the bond formation process step by step. By ramping the current up to 100 nA at 250 mV sample bias, we were able to reproducibly pick up a CO molecule from Cu(CO)₂ and leave

behind Cu(CO) on the surface. However, picking up the remaining CO from Cu(CO) was not as controlled. We were able to break the Cu-CO bond at 100 nA and 500 mV, but the CO molecule usually ended up on the Ag surface rather than on the tip. This higher threshold for breaking the Cu-CO bond is likely to be due to the stronger bond strength compared to the (CO)Cu-CO bond. In comparison, Fe-CO and (CO)Fe-CO bonds could not be broken with voltages up to 1 V at 100 nA.

We have demonstrated the use of STM as a chemical reactor and analyzer of atomic dimensions. These experiments realize the concept of chemical synthesis and structural determination from the bottom up and offer the possibility of understanding complex systems from the properties of their constituents: individual atoms and molecules.

This research was supported by the Division of Chemical Sciences, Office of Basic Energy Sciences, Office of Energy Research, U.S. Department of Energy Grant DE-FG02-91ER14205.

*Corresponding author. Email: wilsonho@ccmr.cornell.edu

¹G. Dujardin, R. E. Walkup, and Ph. Avouris, *Science* **255**, 1232 (1992).

²R. Martel, Ph. Avouris, and I.-W. Lyo, *Science* **272**, 385 (1996).

³B. C. Stipe, M. A. Rezaei, W. Ho, S. Gao, M. Persson, and B. I. Lundqvist, *Phys. Rev. Lett.* **78**, 4410 (1997).

⁴J. Gaudio, H. J. Lee, and W. Ho, *J. Am. Chem. Soc.* **121**, 8479 (1999).

⁵L. J. Lauhon and W. Ho, *Phys. Rev. Lett.* **84**, 1527 (2000).

⁶H. J. Lee and W. Ho, *Science* **286**, 1719 (1999).

⁷B. C. Stipe, M. A. Rezaei, and W. Ho, *Science* **280**, 1732 (1998).

⁸D. M. Eigler and E. K. Schweizer, *Nature (London)* **344**, 524 (1990).

⁹M. F. Crommie, C. P. Lutz, and D. Eigler, *Science* **262**, 218 (1993).

¹⁰L. Bartels, G. Meyer, and K.-H. Rieder, *Phys. Rev. Lett.* **79**, 697

(1997).

¹¹The STM is a variation of the one described in B. C. Stipe, M. A. Rezaei, and W. Ho, *Rev. Sci. Instrum.* **70**, 137 (1999).

¹²In addition to Cu ($4s^13d^{10}$) and Fe ($4s^23d^6$), we have also tried to form gadolinium (Gd: $6s^25d^14f^7$) carbonyl. However, CO molecules always ended up bonding to the Ag surface away from the Gd atom.

¹³During each scan, the sample bias was ramped up and back down in 2.5 mV/step with a dwell time of 300 ms/step. For the present study involving CO vibrations, spectra centered at zero bias were averaged over about 5 scans. The decreased signal-to-noise ratio for the C-O stretch required typically over 100 scans for spectra at the higher bias.

¹⁴L. J. Lauhon and W. Ho, *Phys. Rev. B* **60**, R8525 (1999).

¹⁵R. Fournier, *J. Chem. Phys.* **99**, 1801 (1993).